

Predicting the Number of Future Events

Qinglong Tian, Fanqi Meng, Daniel J. Nordman, William Q. Meeker

Department of Statistics, Iowa State University, Ames, IA 50011

April 9, 2024

This paper describes prediction methods for the number of future events from a population of units associated with an on-going time-to-event process. Examples include the prediction of warranty returns and the prediction of the number of future product failures that could cause serious threats to property or life. Important decisions such as whether a product recall should be mandated are often based on such predictions. Data, generally right-censored (and sometimes left truncated and right-censored), are used to estimate the parameters of a time-to-event distribution. This distribution can then be used to predict the number of events over future periods of time. Such predictions are sometimes called within-sample predictions and differ from other prediction problems considered in most of the prediction literature. This paper shows that the plug-in (also known as estimative or naive) prediction method is not asymptotically correct (i.e., for large amounts of data, the coverage probability always fails to converge to the nominal confidence level). However, a commonly used prediction calibration method is shown to be asymptotically correct for within-sample predictions, and two alternative predictive-distribution-based methods that perform better than the calibration method are presented and justified.

Keywords: Binomial predictand; Bootstrap; Calibration; Censored data; Predictive distribution

1 Introduction

There are many applications where it is necessary to predict the number of future events from a population of units associated with an on-going time-to-event process. Such applications also require a prediction interval to quantify statistical prediction uncertainty arising from the combination of process variability and parameter uncertainty. Some motivating applications are given below.

Product-A Data: This example is from Escobar and Meeker (1999), where, during a particular month, $n=10000$ units of Product-A were put into service. Over the next 48 months, 80 failures occurred and the failure times were recorded. A prediction interval on the number of failures among the remaining 9920 units during the next 12 months was requested by the management.

Heat Exchanger Tube Data: This example is based on data described in Nelson (2000). Nuclear power plants have steam generators that contain many stainless steel heat-exchanger tubes. Cracks initiate and grow in the tubes due to a stress-corrosion mechanism over time. Periodic inspections of the tubes are used to detect cracks. Consider a fleet of steam generators having a total of $n=20,000$ tubes. One crack was detected after the first year of operation, which was followed by another crack during the second year and six more cracks during the third year. The data are interval-censored as the exact initiation times are unknown. A prediction interval was needed for the number of tubes that would crack from the end of the third year to the end of the tenth year.

Bearing-Cage Data: The bearing-cage failure-time data are from Abernethy et al. (1983) and are provided in the online supplementary material. Groups of aircraft engines employing this bearing cage were put into service over time (staggered entry). At the data freeze date, 6 bearing-cage failures had occurred while the remaining 1697 units with various service times were still in service (multiple right-censored data). To assure that a sufficient number of spare parts would be available to repair the aircraft engine in a timely manner, management requested a prediction interval for the number of bearing-cages that would fail in the next year, assuming 300 hours of service for each aircraft.

The purpose of this paper is to show how to construct prediction intervals for the number of future events from an on-going time-to-event process, investigate the properties of different

prediction methods, and give recommendations on which methods to use.

This paper is organized as follows. Section 2 provides concepts and background for prediction inference. Section 3 describes the single-cohort within-sample prediction problem. Section 4 defines how the within-sample prediction is irregular and demonstrates that the plug-in method fails to provide an asymptotically correct prediction interval. Section 5 describes the calibration method for prediction intervals and establishes its asymptotic correctness. Section 6 presents two other prediction interval methods based on predictive distributions. The first one is a general method using parametric bootstrap samples, while the second method is inspired by generalized pivotal quantities and applies to a log-location-scale family of distributions. Section 7 extends the single-cohort within-sample prediction to the multiple-cohort problem. Section 8 compares different prediction methods, through simulation, while Section 9 applies the prediction methods to the motivating examples. Section 10 discusses the choice of distribution for the time-to-event process and addresses the issue of distribution misspecification. Section 11 gives recommendations and describes potential areas for future research.

2 Background

In a general prediction problem, denote the observable data by \mathbf{D}_n and the future random variable by $Y_n \equiv Y$; while generic for now, later this paper will focus on the within-sample prediction where Y is a count. The conditional cdf for Y given \mathbf{D}_n is denoted by $G_n(\cdot|\mathbf{D}_n; \boldsymbol{\theta}) \equiv G(\cdot|\mathbf{D}_n; \boldsymbol{\theta})$, where $\boldsymbol{\theta}$ is a vector of parameters. The goal is to make inference for Y through a prediction interval, as a useful tool for quantifying uncertainty in prediction.

2.1 Prediction Intervals

When parameters in $\boldsymbol{\theta}$ are known, the one-sided upper $100(1 - \alpha/2)\%$ prediction bound $\tilde{Y}_{1-\alpha/2}$ is defined as the $100(1 - \alpha/2)\%$ quantile of the conditional cdf for Y , which is

$$\tilde{Y}_{1-\alpha/2} = \inf\{y \in \mathbb{R} : G(y|\mathbf{D}_n; \boldsymbol{\theta}) = \Pr(Y \leq y|\mathbf{D}_n, \boldsymbol{\theta}) \geq 1 - \alpha/2\}, \quad (1)$$

and the one-sided lower $100(1 - \alpha/2)\%$ prediction bound may be defined as

$$\underline{Y}_{1-\alpha/2} = \sup\{y \in \mathbb{R} : \Pr(Y \geq y|\mathbf{D}_n, \boldsymbol{\theta}) \geq 1 - \alpha/2\}, \quad (2)$$

where this modification of the usual $\alpha/2$ quantile of Y ensures that $\Pr(Y \geq \tilde{Y}_{1-\alpha/2} | \mathbf{D}_n, \boldsymbol{\theta})$ is at least $100(1 - \alpha/2)\%$ when Y is a discrete random variable. We may obtain an equal-tail $100(1 - \alpha)\%$ prediction interval (approximate when Y is a discrete random variable) by combining these two prediction bounds.

In most applications, equal-tail prediction intervals are preferred over unequal ones, even though it is sometimes possible to find a narrower prediction interval with unequal tail probabilities. This is because the equal-tail prediction interval can be naturally decomposed into a practical one-sided upper prediction bound and a lower prediction bound where the separate consideration of one-sided bounds is needed when the cost of being outside the prediction bound is much higher on one side than the other.

When the parameters in $\boldsymbol{\theta}$ are unknown, an estimation of $\boldsymbol{\theta}$ from the observed data \mathbf{D}_n is required. The plug-in method, also known as the naive or estimative method (cf. Section 2.3), is to replace $\boldsymbol{\theta}$ with a consistent estimator $\hat{\boldsymbol{\theta}}_n$ in the prediction bounds (1) and (2). The $100(1 - \alpha)\%$ plug-in upper prediction bound is then $\tilde{Y}_{1-\alpha}^{PL} = \inf\{y \in \mathbb{R} : G(y | \mathbf{D}_n; \hat{\boldsymbol{\theta}}_n) \geq 1 - \alpha\}$ while the $100(1 - \alpha)\%$ plug-in lower prediction bound is $\tilde{Y}_{1-\alpha/2}^{PL} = \sup\{y \in \mathbb{R} : \Pr(Y \geq y | \mathbf{D}_n, \hat{\boldsymbol{\theta}}_n) \geq 1 - \alpha\}$.

2.2 Coverage Probability

Besides the plug-in method, other methods for computing prediction bounds or intervals are available. Let $\text{PI}(1 - \alpha)$ generically denote a prediction interval (or bound) of a nominal coverage level $100(1 - \alpha)\%$, where researchers would like the probability of Y falling within the interval to be (or close to) $1 - \alpha$ (i.e., $\Pr[Y \in \text{PI}(1 - \alpha)] = 1 - \alpha$).

To be clear, there are two possible types of coverage probability: conditional coverage probability and unconditional (overall) coverage probability. The conditional coverage probability of a particular $\text{PI}(1 - \alpha)$ method is defined as

$$\text{CP}[\text{PI}(1 - \alpha) | \mathbf{D}_n; \boldsymbol{\theta}] = \Pr[Y \in \text{PI}(1 - \alpha) | \mathbf{D}_n; \boldsymbol{\theta}],$$

where $\Pr(\cdot | \mathbf{D}_n; \boldsymbol{\theta})$ denotes the conditional probability of Y given the observable data \mathbf{D}_n . The conditional coverage probability $\text{CP}[\text{PI}(1 - \alpha) | \mathbf{D}_n; \boldsymbol{\theta}]$ is a random variable because it is a function of the data \mathbf{D}_n . The unconditional coverage probability of a prediction interval

method can be obtained by taking an expectation with respect to the data \mathbf{D}_n and it is defined as

$$\text{CP}[\text{PI}(1 - \alpha); \boldsymbol{\theta}] = \mathbf{E} \{ \Pr[Y \in \text{PI}(1 - \alpha) | \mathbf{D}_n; \boldsymbol{\theta}] \}.$$

The unconditional coverage probability is a fixed property of a prediction method and, as such, can be most readily studied and used to compare alternative prediction interval methods. We focus on unconditional coverage probability in this paper and use the term coverage probability to refer to the unconditional probability, unless stated otherwise.

We say a prediction method is exact if $\text{CP}[\text{PI}(1 - \alpha); \boldsymbol{\theta}] = 1 - \alpha$ holds. If $\text{CP}[\text{PI}(1 - \alpha); \boldsymbol{\theta}]$ converges to $1 - \alpha$ as the sample size n increases, we say the corresponding prediction method is asymptotically correct. When Y is a discrete random variable, however, asymptotic correctness and exactness may not generally hold or be possible for a prediction interval method, due to the discreteness in the distribution of Y .

2.3 Related Literature

Extensive research exists regarding some methods for computing prediction intervals. While the plug-in method has been criticized for ignoring the uncertainty in $\hat{\boldsymbol{\theta}}_n$, this method is often widely viewed as being asymptotically correct (related to “regular predictions” described in Section 4.1). For example, Cox (1975), Beran (1990), and Hall et al. (1999) showed that the coverage probability of the plug-in method has an accuracy of $O(n^{-1})$ for a continuous predictand under certain conditions. In Section 4 we show, however, that the plug-in method is not asymptotically correct in the context of within-sample prediction.

Section 5 presents a calibration method for within-sample prediction intervals. Cox (1975) originally proposed the calibration idea to improve on the plug-in method and also provided analytical forms for prediction intervals based on general asymptotic expansions. Atwood (1984) used a similar method. Beran (1990) employed bootstrap in the calibration method, avoiding the complicated analytical expressions. Escobar and Meeker (1999) described similar methods for constructing prediction intervals for failure times and the number of future failures, based on censored life data.

This paper does not specifically address Bayesian prediction methods, but the classic idea

of a Bayesian predictive distribution can be extended to non-Bayesian methods and two such methods are considered in Section 6. Several authors have considered similar notions of a non-Bayesian predictive distribution (e.g., Aitchison (1975), Davison (1986), Barndorff-Nielsen and Cox (1996)). Lawless and Fredette (2005) demonstrated a relationship between predictive distributions and (approximate) pivotal-based prediction intervals, including the calibration method described in Beran (1990). Fonseca et al. (2012) further elaborated on the relationship between predictive distributions and the calibration method. Shen et al. (2018) proposed a general framework to construct a predictive distribution by replacing the posterior distribution in the definition of a Bayesian predictive distribution with a confidence distribution.

3 Single Cohort Within-Sample Prediction

3.1 Within-Sample Prediction and New Sample Prediction

The term “within-sample” prediction has been used to distinguish from the more widely known “new sample” prediction. In new-sample prediction, past data are used, for example, to compute a prediction interval for the lifetime of a single unit from a new and completely independent sample. For within-sample prediction, however, the sample has not changed; the future random variable that researchers wish to predict (i.e., a count) relates to the same sample that provided the original (censored) data.

3.2 Single-Cohort Within-Sample Prediction and Plug-in Method

Let (T_1, \dots, T_n) be an unordered random sample from a parametric distribution $F(t; \theta)$ having support on the positive real line and $\theta \in \mathbb{R}^q$. Under Type I censoring at $t_c > 0$, the available data may then be expressed by $D_i = (\delta_i, T_i^{obs}), i = 1, \dots, n$, where $\delta_i = I(T_i \leq t_c)$ is a variable indicating whether T_i is observed before the censoring time t_c , so that the actual observed variables are given as $T_i^{obs} = T_i \delta_i + t_c(1 - \delta_i)$. The observed number of events (uncensored units) in the sample will be denoted by $r_n = \sum_{i=1}^n I(T_i \leq t_c)$. For a future time $t_w > t_c$, let $Y_n = \sum_{i=1}^n I(T_i \in (t_c, t_w])$ denote the (future) number of values from T_1, \dots, T_n , that occur in the interval $(t_c, t_w]$. The conditional distribution of Y_n is then binomial($n - r_n, p$) given the observed data $\mathbf{D}_n = (D_1, \dots, D_n)$, where p is the conditional probability that $T_i \in (t_c, t_w]$ given

that $T_i > t_c$. As a function of θ , we may define p by

$$p \equiv \pi(\theta) = \frac{F(t_w; \theta) - F(t_c; \theta)}{1 - F(t_c; \theta)}. \quad (3)$$

The goal is to construct a prediction interval for Y_n based on the observed data $\mathbf{D}_n = (D_1, \dots, D_n)$ when θ is unknown. This is referred to as single-cohort within-sample prediction because all the units enter the system at the same time and are homogeneous; and both the data \mathbf{D}_n and the predictand Y_n are functions of the uncensored random sample (T_1, \dots, T_n) .

Let $\hat{\theta}_n$ denote an estimator of θ based on \mathbf{D}_n , then a plug-in estimator $\hat{p}_n = \pi(\hat{\theta}_n)$ of the conditional probability p follows from (3). Analogous to the bounds in Section 2.1, a $100(1 - \alpha)\%$ plug-in lower prediction bound is defined as

$$\begin{aligned} \tilde{Y}_{n,1-\alpha}^{PL} &= \sup\{y \in \{0\} \cup \mathbb{Z}^+; \text{pbinom}(y - 1, n - r_n, \hat{p}_n) \leq \alpha\} \\ &= \begin{cases} \text{qbinom}(\alpha, n - r_n, \hat{p}_n), & \text{if } \text{pbinom}(\text{qbinom}(\alpha, n - r_n, \hat{p}_n), n - r_n, \hat{p}_n) > \alpha. \\ \text{qbinom}(\alpha, n - r_n, \hat{p}_n) + 1, & \text{if } \text{pbinom}(\text{qbinom}(\alpha, n - r_n, \hat{p}_n), n - r_n, \hat{p}_n) = \alpha. \end{cases} \end{aligned}$$

where pbinom and qbinom are, respectively, the binomial cdf and quantile function. Similarly, the $100(1 - \alpha)\%$ plug-in upper prediction bound for Y_n is defined as

$$\tilde{Y}_{n,1-\alpha}^{PL} = \inf\{y \in \{0\} \cup \mathbb{Z}^+; \text{pbinom}(y, n - r_n, \hat{p}_n) \geq 1 - \alpha\} = \text{qbinom}(1 - \alpha, n - r_n, \hat{p}_n).$$

Section 2.2 mentioned that asymptotically correct coverage may not generally be possible for prediction intervals involving a discrete predictand. However, for within-sample prediction here, prediction interval methods can be sensibly examined for properties of asymptotic correctness, which we consider in the following section. This is because discreteness in the (conditionally) binomial predictand Y_n essentially disappears in large sample sizes n , due to normal approximations.

4 The Irregularity of the Within-Sample Prediction

4.1 A Regular Prediction Problem

Under the general prediction framework described in Section 2, the conditional cdf $G_n(\cdot | \mathbf{D}_n; \theta)$ of a predictand Y_n given the observed data \mathbf{D}_n is often estimated by the plug-in method as $G_n(\cdot | \mathbf{D}_n; \hat{\theta}_n)$ (also known as a predictive distribution), where $\hat{\theta}_n$ is a consistent estimator of

θ based on D_n . To frame much of the literature related to the plug-in method (Section 2.3), we may define the prediction problem most often commonly related to the plug-in method as “regular” according to the following definition.

Definition 1. In the notation of Section 2, a prediction problem is called regular if

$$\sup_{y \in \mathbb{R}} |G_n(y|D_n; \theta) - G_n(y|D_n; \hat{\theta}_n)| \xrightarrow{p} 0$$

holds as $n \rightarrow \infty$ for any consistent estimator $\hat{\theta}_n$ of θ (i.e., $\hat{\theta}_n \xrightarrow{p} \theta$).

Unlike coverage probability (where exactness may again not be possible for discrete predictands), the above definition reflects the underlying sense of how the plug-in method for prediction intervals is often asymptotically valid for both discrete and continuous predictands. By the nature of many prediction problems (e.g., new sample prediction), the conditional form of cdf G_n may also not necessarily vary with n (e.g., $G_n(\cdot|D_n; \theta) = G(\cdot; \theta)$). Hence, in a regular prediction problem, the plug-in predictive distribution (estimated cdf) asymptotically captures the true conditional cdf of the predictand, so that differences are expected to vanish between quantiles of the true predictand Y_n and the associated plug-in prediction bounds. Further, when the predictand has a continuous and asymptotically tight conditional distribution (with probability 1), such as when the conditional cdf $G_n(\cdot|D_n; \theta) = G(\cdot; \theta)$ of the predictand does not vary with n , then the plug-in method will be asymptotically correct.

4.2 Failure of the Plug-in Method

This section shows that the within-sample prediction problem described in Section 3 is not regular and that the plug-in method is not asymptotically valid for within-sample prediction. To avoid redundancy, the presentation of results will focus on the plug-in upper prediction bound; the lower bound is analogous by Remark 1 below. In the context of within-sample prediction (cf. Section 3.2), recall that the $100(1 - \alpha)\%$ plug-in upper prediction bound for the future count $Y_n \equiv \sum_{i=1}^n I(T_i \in (t_c, t_w])$ is defined as

$$\tilde{Y}_{n,1-\alpha}^{PL} = \inf\{y \in \mathbb{Z}; \text{pbinom}(y, n - r_n, \hat{p}_n) \geq 1 - \alpha\}.$$

The following theorem shows that the coverage probability of $\tilde{Y}_{n,1-\alpha}^{PI}$ will not correctly converge to $1 - \alpha$ as n increases.

Theorem 1. Let T_1, \dots, T_n denote a random sample from a parametric distribution with cdf $F(\cdot; \boldsymbol{\theta}_0)$ (at the true value of $\boldsymbol{\theta} = \boldsymbol{\theta}_0 \in \mathbb{R}^q$), which is observed under Type I censoring at $t_c > 0$. Suppose also that $F(t_c; \boldsymbol{\theta}_0) < 1$, $p_0 = \pi(\boldsymbol{\theta}_0) \in (0, 1)$ in (3), $F(t_c; \boldsymbol{\theta})$ is continuous at $\boldsymbol{\theta}_0$, and that the conditional probability (parametric function) $p \equiv \pi(\boldsymbol{\theta})$ is continuously differentiable in a neighborhood of $\boldsymbol{\theta}_0$ with non-zero gradient $\nabla_0 \equiv \partial\pi(\boldsymbol{\theta})/\partial\boldsymbol{\theta}|_{\boldsymbol{\theta}=\boldsymbol{\theta}_0}$. Based on the censored sample, suppose $\hat{\boldsymbol{\theta}}_n$ is an estimator of $\boldsymbol{\theta}$ satisfying $\sqrt{n}(\hat{\boldsymbol{\theta}}_n - \boldsymbol{\theta}_0) \xrightarrow{d} \text{MVN}(\mathbf{0}, \mathbf{V}_0)$, as $n \rightarrow \infty$, for a multivariate normal distribution with mean vector $\mathbf{0}$ and positive definite variance matrix \mathbf{V}_0 . Then,

1. The within-sample prediction of $Y_n = \sum_{i=1}^n \mathbf{I}(t_c < T_i \leq t_w)$ fails to be a regular prediction problem: denoting $G_n(y|\mathbf{D}_n, \boldsymbol{\theta}_0) = \text{pbinom}(y, n - r_n, p_0)$ as the conditional cdf of Y_n and $G_n(y|\mathbf{D}_n, \hat{\boldsymbol{\theta}}_n) = \text{pbinom}(y, n - r_n, \hat{p}_n)$ as its plug-in estimator, then

$$\sup_{y \in \mathbb{R}} \left| G_n(y|\mathbf{D}_n, \boldsymbol{\theta}_0) - G_n(y|\mathbf{D}_n, \hat{\boldsymbol{\theta}}_n) \right| \xrightarrow{d} 1 - 2\Phi_{\text{nor}}(\sqrt{v_1}|Z_1|/2),$$

where Z_1 is a standard normal variable with cdf $\Phi_{\text{nor}}(z) = \int_{-\infty}^z 1/\sqrt{2\pi}e^{-u^2/2}du$, $z \in \mathbb{R}$, and

$$v_1 \equiv \frac{[1 - F(t_c; \boldsymbol{\theta}_0)]}{p_0(1 - p_0)} \nabla_0^t \mathbf{V}_0 \nabla_0 \in (0, \infty).$$

2. The plug-in upper prediction bound $\tilde{Y}_{n,1-\alpha}^{PL}$ generally fails to have asymptotically correct coverage:

$$\lim_{n \rightarrow \infty} \Pr(Y_n \leq \tilde{Y}_{n,1-\alpha}^{PL}) = \Lambda_{1-\alpha}(v_1) \in (0, 1) \quad \text{such that}$$

$$\text{sgn} [\Lambda_{1-\alpha}(v_1) - (1 - \alpha)] = \begin{cases} 1 & \text{if } \alpha \in (1/2, 1) \\ 0 & \text{if } \alpha = 1/2 \\ -1 & \text{if } \alpha \in (0, 1/2), \end{cases}$$

where $\text{sgn}(\cdot)$ is the sign function and $\Lambda_{1-\alpha}(v_1) \equiv \int_{-\infty}^{\infty} \Phi_{\text{nor}}^{-1}(1 - \alpha) + z\sqrt{v_1} \, d\Phi_{\text{nor}}(z)$.

Furthermore, $\Lambda_{1-\alpha}(v_1) \in [1/2, 1 - \alpha)$ is a decreasing function of $v_1 > 0$ for a given $\alpha \in (0, 1/2)$, while $\Lambda_{1-\alpha}(v_1) \in (1 - \alpha, 1/2]$ is increasing in $v_1 > 0$ for $\alpha \in (1/2, 1)$, and $\lim_{v_1 \rightarrow \infty} \Lambda_{1-\alpha}(v_1) = 1/2$ holds for any $\alpha \in (0, 1)$.

Remark 1. The lower plug-in bound $\tilde{Y}_{n,1-\alpha}^{PL}$ behaves similarly with $\lim_{n \rightarrow \infty} \Pr(Y_n \geq \tilde{Y}_{n,1-\alpha}^{PL}) = \lim_{n \rightarrow \infty} \Pr(Y_n \leq \tilde{Y}_{n,1-\alpha}^{PL})$ in Theorem 1.

The proof of Theorem 1 is in the online supplementary material. This counter-intuitive result reveals that the plug-in method should not be used to construct prediction intervals in the within-sample prediction problem, even if the sample size is large. The first part of Theorem 1 entails that plug-in estimation fails to capture the distribution of the predictand Y_n here, to the extent that the supremum difference between estimated and true distributions has a *random* limit, rather than converging to zero as in a regular prediction (cf. Definition 1). As a consequence, the limiting coverage probability of the plug-in bound turns out to be “off” by an amount determined by a magnitude of $v_1 > 0$ in Theorem 1 (part 2). For increasing values of v_1 , the coverage probability approaches 0.5, regardless of the nominal coverage level intended. An intuitive explanation for the failure of plug-in method is that, although \hat{p}_n converges consistently to p , the growing number of Bernoulli trials $n - r_n$ in Y_n offsets the improvements that larger samples may offer in estimation by \hat{p}_n . In other words, when standardizing the true $1 - \alpha$ quantile, say $Y_{n,1-\alpha}$, of the (conditionally binomial) predictand Y_n , one obtains a standard normal quantile $(Y_{n,1-\alpha} - p)/\sqrt{n - r_n} \approx \Phi_{\text{nor}}^{-1}(1 - \alpha)$ by normal approximation; however, the same standardization applied to the plug-in bound $\tilde{Y}_{n,1-\alpha}^{PL}$ gives $(\tilde{Y}_{n,1-\alpha}^{PL} - p)/\sqrt{n - r_n} \approx \Phi_{\text{nor}}^{-1}(1 - \alpha) + \sqrt{n - r_n}(\hat{p}_n - p)$, which differs by a substantial and random amount $\sqrt{n - r_n}(\hat{p}_n - p)$ (having a normal limit itself). Hence, validity of the plug-in method for within-sample prediction would require an estimator \hat{p}_n such that $\hat{p}_n = p + o_p(n^{-1/2})$, which demands more than what is available from standard \sqrt{n} -consistency.

5 Prediction Intervals Based on Calibration

5.1 Calibrating Plug-in Prediction Bounds

Cox (1975) suggested an approximation for improving the plug-in method, which will be described next. Considering the general prediction problem (cf. Section 2.1), suppose a future random variable $Y \equiv Y_n$ has a conditional cdf $G_n(\cdot | \mathbf{D}_n; \boldsymbol{\theta}) \equiv G(\cdot | \mathbf{D}_n; \boldsymbol{\theta})$ given random sample \mathbf{D}_n and $\hat{\boldsymbol{\theta}}_n$ is a consistent estimator of $\boldsymbol{\theta}$ from \mathbf{D}_n . The coverage probability of the $100(1 - \alpha)\%$ plug-in upper prediction bound is denoted by $\Pr \left[G(Y | \mathbf{D}_n; \hat{\boldsymbol{\theta}}_n) \leq 1 - \alpha \right] = 1 - \alpha'$, where α' is generally different from α due to the estimation uncertainty in $\hat{\boldsymbol{\theta}}_n$. The basic idea of the calibration method is to find a level α^\dagger so that the coverage probability $\Pr \left[G(Y | \mathbf{D}_n; \hat{\boldsymbol{\theta}}_n) \leq 1 - \alpha^\dagger \right]$

is equal to (or closer to) $1 - \alpha$. The resulting $100(1 - \alpha^\dagger)\%$ upper plug-in prediction bound $\tilde{Y}_{n,1-\alpha^\dagger}^{PL}$ is called the $100(1 - \alpha)\%$ upper calibrated prediction bound. However, determination of α^\dagger relies on both the distribution of Y and the sampling distribution of $\hat{\theta}_n$, each of which depends on the unknown parameter θ . So instead, α^\dagger is obtained by solving the equation $\Pr_* \left[G(Y^* | \mathbf{D}_n; \hat{\theta}_n^*) \leq 1 - \alpha^\dagger \right] = 1 - \alpha$, where \Pr_* denotes bootstrap probability induced by $Y^* \sim G(\cdot | \mathbf{D}_n; \hat{\theta}_n)$ and by $\hat{\theta}_n^*$ as a bootstrap version of $\hat{\theta}_n$; for example, $\hat{\theta}_n^*$ may be based on a bootstrap sample \mathbf{D}_n^* found by a parametric bootstrap applied using $\hat{\theta}_n$ in the role of the unknown parameter vector θ . Beran (1990) showed, that under certain conditions, instead of having a coverage error of $O(n^{-1})$, the coverage probability of the calibrated upper prediction bound improves upon the plug-in methods, e.g., $\Pr \left[Y \leq G^{-1}(1 - \alpha^\dagger | \mathbf{D}_n; \hat{\theta}_n) \right] = 1 - \alpha + O(n^{-2})$. However, such results for the validity of the calibration method cannot be applied directly to within-sample prediction because conditions in Beran (1990) entail that the prediction problem be regular (cf. Section 4.1), which is not true for the within-sample prediction problem (Theorem 1). Consequently, the issue of asymptotic correctness for the calibration method needs to be determined for within-sample prediction, as next considered.

5.2 The Calibration-Bootstrap Method for the Within-Sample Prediction

The general method in Beran (1990) is modified to construct a calibrated prediction interval for within-sample prediction and it is called the calibration-bootstrap method in the rest of this paper. For a bootstrap sample \mathbf{D}_n^* with r_n^* observed events (e.g., from a parametric bootstrap using $\hat{\theta}_n$), we define a random variable set $(Y_n^\dagger, n - r_n^*, \hat{p}_n^*)$ where $\hat{p}_n^* = \pi(\hat{\theta}_n^*)$ is the bootstrap version of $\hat{p}_n = \pi(\hat{\theta}_n)$ and $Y_n^\dagger \sim \text{binomial}(n - r_n^*, \hat{p}_n^*)$, conditional on r_n^* .

For the $100(1 - \alpha)\%$ lower prediction bound, the calibrated confidence level is

$$\alpha_L^\dagger = \sup\{u \in [0, 1] : \Pr_* [\text{pbinom}(Y_n^\dagger, n - r_n^*, \hat{p}_n^*) \leq u] \leq \alpha\},$$

where \Pr_* is the bootstrap probability induced by \mathbf{D}_n^* , and then the calibrated $100(1 - \alpha)\%$ lower prediction bound is given by $\underline{Y}_{n,1-\alpha}^C = \underline{Y}_{n,1-\alpha_L^\dagger}^{PL}$. For the $100(1 - \alpha)\%$ upper prediction bound, the calibrated confidence level is

$$1 - \alpha_U^\dagger = \inf\{u \in [0, 1] : \Pr_* [\text{pbinom}(Y_n^\dagger, n - r_n^*, \hat{p}_n^*) \leq u] \geq 1 - \alpha\},$$

so that the calibrated $100(1 - \alpha)\%$ upper prediction bound is $\tilde{Y}_{n,1-\alpha}^C = \tilde{Y}_{n,1-\alpha_U}^{PL}$. Here $\tilde{Y}_{n,1-\alpha}^{PL}$ and $\tilde{Y}_{n,1-\alpha}^{PL}$ represent lower and upper plug-in prediction bounds, respectively, as defined in Section 3.2.

The calibration-bootstrap method involves approximating the distribution of $U = \text{pbinom}(Y_n, n - r_n, \hat{p}_n)$ with the bootstrap distribution of $U^* = \text{pbinom}(Y_n^\dagger, n - r_n^*, \hat{p}_n^*)$. The bootstrap distribution of U^* is used to calibrate the plug-in method. The procedure of using the calibration-bootstrap method to construct a prediction interval is described below:

1. Compute the maximum likelihood (ML) estimate $\hat{\theta}_n$ using data D_n and the ML estimate $\hat{p}_n = \pi(\hat{\theta}_n)$.
2. Generate a bootstrap sample D_n^* and the number of events is denoted by r_n^* .
3. Compute $\hat{\theta}_n^*$ and $\hat{p}_n^* = \pi(\hat{\theta}_n^*)$ using the bootstrap sample D_n^* .
4. Generate y^* from the distribution $\text{binomial}(n - r_n^*, \hat{p}_n^*)$ and compute $u^* = \text{pbinom}(y^*, n - r_n^*, \hat{p}_n^*)$.
5. Repeat step 2-4 for B times and get B realizations of u^* as $\{u_1^*, \dots, u_B^*\}$.
6. Find the α and $1 - \alpha$ quantiles of $\{u_1^*, \dots, u_B^*\}$, and denote these by u_α and $u_{1-\alpha}$, respectively. The $1 - \alpha$ calibrated lower and upper prediction bounds are $\tilde{Y}_{n,1-\alpha}^C = \tilde{Y}_{n,1-u_\alpha}^{PL}$ and $\tilde{Y}_{n,1-\alpha}^C = \tilde{Y}_{n,u_{1-\alpha}}^{PL}$.

The pseudo-code for this algorithm is in the online supplementary material.

Next, the calibration-bootstrap method is shown to be asymptotically correct. This requires a mild assumption on the bootstrap involved, namely that the parameter estimators $\hat{\theta}_n^*$ in the bootstrap world provide valid approximations for the sampling distribution of the original data estimators $\sqrt{n}(\hat{\theta}_n - \theta)$, in large samples. More formally, let $\mathcal{L}_n^* \equiv \mathcal{L}_n^*(D_n)$ denote the probability law of the bootstrap quantity $\sqrt{n}(\hat{\theta}_n^* - \hat{\theta}_n)$ (conditional on the data D_n) and let \mathcal{L}_n denote the probability law of $\sqrt{n}(\hat{\theta}_n - \theta)$. Let $\rho(\mathcal{L}_n, \mathcal{L}_n^*)$ denote the distance between these distributions under any metric $\rho(\cdot, \cdot)$ that metricizes the topology of weak convergence (e.g., the Prokhorov Metric). Also, in the bootstrap re-creation, the probability $\Pr_*(T_1^* \leq t_c)$ that a bootstrap observation T_1^* is observed before the censoring time t_c should be a consistent estimator of $F(t_c; \theta)$ (e.g., $\Pr_*(T_1^* \leq t_c) = F(t_c; \hat{\theta}_n)$ would hold as a natural estimator under a parametric bootstrap).

Theorem 2. *Under the conditions of Theorem 1, suppose that $\rho(\mathcal{L}_n^*, \mathcal{L}_n) \xrightarrow{p} 0$ and $\Pr_*(T_1^* \leq t_c) \xrightarrow{p} F(t_c; \boldsymbol{\theta}_0)$ as $n \rightarrow \infty$. Then, the $100(1 - \alpha)\%$ calibrated upper and lower prediction bounds, respectively $\tilde{Y}_{n,1-\alpha}^C$ and $\tilde{Y}_{n,1-\alpha}^C$ have asymptotically correct coverage, that is*

$$\lim_{n \rightarrow \infty} \Pr(Y_n \leq \tilde{Y}_{n,1-\alpha}^C) = 1 - \alpha = \lim_{n \rightarrow \infty} \Pr(Y_n \geq \tilde{Y}_{n,1-\alpha}^C).$$

The proof is in the online supplementary material. Theorem 2 and its extension in Section 7 guarantee, for example, that the calibration prediction method employed in Escobar and Meeker (1999), Hong et al. (2009), Hong and Meeker (2010), and Hong and Meeker (2013) to construct the prediction intervals for the cumulative number of events is asymptotically correct.

6 Prediction Intervals Based on Predictive Distributions

6.1 Predictive Distributions

Under the general prediction setting in Section 2, recall that the predictive distribution under the plug-in method, given by $G(\cdot | \mathbf{D}_n, \hat{\boldsymbol{\theta}}_n)$, provides an estimator of the conditional cdf $G(\cdot | \mathbf{D}_n; \boldsymbol{\theta})$, of the predictand Y . Quantiles of this predictive distribution can be associated with prediction bounds for Y . Generally speaking, any method that leads to a prediction bound for Y can be translated to a predictive distribution by defining the $100(1 - \alpha)\%$ upper prediction bound as the $1 - \alpha$ quantile of the predictive distribution (and vice versa). In this section, the strategy is to construct predictive distributions that lead to prediction bound (or interval) methods having asymptotically correct coverage for within-sample prediction.

For this purpose, it is helpful to consider a Bayesian predictive distribution, defined by

$$G_B(y | \mathbf{D}_n) = \int G(y | \mathbf{D}_n; \boldsymbol{\theta}) \gamma(\boldsymbol{\theta} | \mathbf{D}_n) d\boldsymbol{\theta}, \quad (4)$$

where $\gamma(\boldsymbol{\theta} | \mathbf{D}_n)$ is a joint posterior distribution for $\boldsymbol{\theta}$. The $1 - \alpha$ quantile of the Bayesian predictive distribution provides the $100(1 - \alpha)\%$ upper Bayesian prediction bound. While this paper does not pursue the Bayesian method, the idea of the Bayesian predictive distribution can nevertheless be used by replacing the posterior $\gamma(\boldsymbol{\theta} | \mathbf{D}_n)$ in (4) with an alternative distribution over parameters to similarly define non-Bayesian predictive distributions. Harris (1989)

replaced the posterior distribution in (4) with the bootstrap distribution of the parameters to construct a predictive distribution while Wang et al. (2012) replaced the posterior distribution with a fiducial distribution. Shen et al. (2018) proposed a framework for predictive inference by replacing the posterior distribution in (4) with a confidence distribution (CD) and provided theoretical results for this CD-based predictive distribution for the case of a scalar parameter. A CD is a probability distribution that can quantify the uncertainty of an unknown parameter, where both the bootstrap distribution in Harris (1989) and the fiducial distribution in Wang et al. (2012) can be viewed as CDs; see Xie and Singh (2013) for a review of these ideas.

To summarize, a predictive distribution can be constructed by using a data-based distribution on the parameter space to replace the posterior distribution in (4). Following this idea, we aim to use draws from a joint probability distribution for the parameters such that the resulting predictive distribution can be used to construct asymptotically correct prediction bounds and intervals for within-sample prediction. In particular, we propose two ways of constructing predictive distributions, extending the framework proposed by Shen et al. (2018) to the within-sample prediction case. In Section 6.2, we describe a prediction method that is based on the bootstrap distribution of the parameters and it is called the direct-bootstrap method in this paper. In Section 6.3, we describe another method that works specifically with the (log)-location-scale family of distributions. This method is inspired by generalized pivotal quantities (GPQ) and involves generating bootstrap samples and it is called the GPQ-bootstrap method.

6.2 The Direct-Bootstrap Method

For within-sample prediction, recall that number Y_n of events between the censoring time t_c and a future time $t_w > t_c$, given the Type I censored data \mathbf{D}_n , is $\text{binomial}(n - r_n, p)$, where r_n is the number of events observed in \mathbf{D}_n and p is the conditional probability in (3). The direct-bootstrap method uses the distribution of a bootstrap version $\hat{p}_n^* = \pi(\hat{\theta}_n^*)$ of $\hat{p}_n = \pi(\hat{\theta}_n)$, which is induced by the distribution of estimates $\hat{\theta}_n^*$ from a bootstrap sample \mathbf{D}_n^* , to construct a predictive distribution. Letting Pr_* denote bootstrap probability (probability induced by a bootstrap sample \mathbf{D}_n^*), the predictive distribution constructed using direct-bootstrap method is

$$G_{Y_n}^{DB}(y|\mathbf{D}_n) = \int \text{pbinom}(y, n - r_n, \hat{p}_n^*) \text{Pr}_*(d\hat{p}_n^*) \approx \frac{1}{B} \sum_{b=1}^B \text{pbinom}(y, n - r_n, \hat{p}_b^*), \quad (5)$$

where $\hat{p}_1^*, \dots, \hat{p}_B^*$ are realized bootstrap versions of \hat{p}_n from B independently generated bootstrap samples $\mathbf{D}_n^{*(1)}, \dots, \mathbf{D}_n^{*(B)}$, and B is the number of bootstrap samples. The $100(1 - \alpha)\%$ lower and upper prediction bounds using the direct-bootstrap method are then

$$\begin{aligned} \underline{Y}_{n,1-\alpha}^{DB} &= \sup \{y \in \{0\} \cup \mathbb{Z}^+ : G_{Y_n}^{DB}(y - 1 | \mathbf{D}_n) \leq \alpha\}, \\ \tilde{Y}_{n,1-\alpha}^{DB} &= \inf \{y \in \{0\} \cup \mathbb{Z}^+ : G_{Y_n}^{DB}(y | \mathbf{D}_n) \geq 1 - \alpha\}. \end{aligned} \quad (6)$$

6.3 The GPQ-Bootstrap Method

This section focuses on the log-location-scale distribution family and develops another method to construct a predictive distribution through approximate GPQs. Suppose (T_1, \dots, T_n) is an i.i.d. random sample from a log-location-scale distribution

$$F(t; \mu, \sigma) = \Phi \left[\frac{\log(t) - \mu}{\sigma} \right], \quad (7)$$

where $\Phi(\cdot)$ is a known cdf that is free of parameters. For example, if $\Phi(\cdot)$ is the standard normal cdf $\Phi_{\text{nor}}(\cdot)$, then T_1 has the log-normal distribution.

Hannig et al. (2006) described methods for constructing GPQs and outlined the relationship between GPQs and fiducial inference. Applying these ideas, GPQs can be defined for the parameters (μ, σ) in the log-location-scale model as follows. If \mathbb{S} is a complete or Type II censored independent sample from a log-location-scale distribution, a set of GPQs for (μ, σ) under \mathbb{S} is given by

$$\mu_n^{**} = \hat{\mu}_n + \left(\frac{\mu - \hat{\mu}_n^{\mathbb{S}^*}}{\hat{\sigma}_n^{\mathbb{S}^*}} \right) \hat{\sigma}_n \quad \text{and} \quad \sigma_n^{**} = \left(\frac{\sigma}{\hat{\sigma}_n^{\mathbb{S}^*}} \right) \hat{\sigma}_n, \quad (8)$$

where \mathbb{S}^* denotes an independent copy of the sample \mathbb{S} , and $(\hat{\mu}_n, \hat{\sigma}_n)$ and $(\hat{\mu}_n^{\mathbb{S}^*}, \hat{\sigma}_n^{\mathbb{S}^*})$ denote the ML estimators of (μ, σ) computed from \mathbb{S} and \mathbb{S}^* , respectively. These GPQs induce a distribution over the parameter space (μ, σ) based on data estimates $(\hat{\mu}_n, \hat{\sigma}_n)$ and, due to the fact that $[(\mu - \hat{\mu}_n)/\sigma, \hat{\sigma}_n/\sigma]$ are pivotal quantities based on a complete or Type II censored sample T_1, \dots, T_n from the log-location-family, the distribution of $[(\mu - \hat{\mu}_n^{\mathbb{S}^*})/\hat{\sigma}_n^{\mathbb{S}^*}, \sigma/\hat{\sigma}_n^{\mathbb{S}^*}]$ in (8) can be directly approximated by simulation.

GPQs can also, in some applications, be used to construct confidence intervals when an exact pivot is unavailable. Notice that, while the quantities in (8) are GPQs for log-location-scale family based on complete or Type II censored data, these are no longer GPQs with Type I

censored data, where exact GPQs technically fail to exist. This is because the distribution of $[(\mu - \hat{\mu}_n)/\hat{\sigma}_n, \sigma/\hat{\sigma}_n]$ depends on the unknown event probability $F(t_c; \mu, \sigma)$ before the censoring time t_c under Type I censoring, which applies also to $[(\mu - \hat{\mu}_n^{S*})/\hat{\sigma}_n^{S*}, \sigma/\hat{\sigma}_n^{S*}]$.

However, the formula in (8) can be used to provide a joint approximate GPQ distribution under Type I censoring. Letting $\hat{\theta}_n^* = (\hat{\mu}_n^*, \hat{\sigma}_n^*)$ denote a bootstrap version of $\hat{\theta}_n = (\hat{\mu}_n, \hat{\sigma}_n)$, (8) is extended to define a joint approximate GPQ distribution as the bootstrap distribution of $\hat{\theta}_n^{**} = (\hat{\mu}_n^{**}, \hat{\sigma}_n^{**})$, where

$$\hat{\mu}_n^{**} = \hat{\mu}_n + \left(\frac{\hat{\mu}_n - \hat{\mu}_n^*}{\hat{\sigma}_n^*} \right) \hat{\sigma}_n \quad \text{and} \quad \hat{\sigma}_n^{**} = \left(\frac{\hat{\sigma}_n}{\hat{\sigma}_n^*} \right) \hat{\sigma}_n. \quad (9)$$

The above definition of $\hat{\theta}_n^{**}$ also follows by using the bootstrap distribution of $[(\hat{\mu}_n - \hat{\mu}_n^*)/\hat{\sigma}_n^*, \hat{\sigma}_n/\hat{\sigma}_n^*]$ to approximate the sampling distribution of $[(\mu - \hat{\mu}_n)/\hat{\sigma}_n, \sigma/\hat{\sigma}_n]$ and linearly solving for (μ, σ) . Then using $\hat{\theta}_n^{**} = (\hat{\mu}_n^{**}, \hat{\sigma}_n^{**})$ instead of $\hat{\theta}_n^* = (\hat{\mu}_n^*, \hat{\sigma}_n^*)$, a predictive distribution can be defined by using the same procedure that defined the predictive distribution in (5). Namely, by defining a random variable $\hat{p}_n^{**} \equiv \pi(\hat{\theta}_n^{**})$ from (3) with a bootstrap distribution induced by $\hat{\theta}_n^{**} = (\hat{\mu}_n^{**}, \hat{\sigma}_n^{**})$, the predictive distribution for Y_n using the GPQ-bootstrap method is given by

$$G_{Y_n}^{GPQ}(y|\mathbf{D}_n) = \int \text{pbinom}(y, n - r_n, \hat{p}_n^{**}) \Pr_*(d\hat{p}_n^{**}) \approx \frac{1}{B} \sum_{b=1}^B \text{pbinom}(y, n - r_n, \hat{p}_b^{**}),$$

where $\hat{p}_1^{**}, \dots, \hat{p}_B^{**}$ are computed from realized bootstrap samples. The $100(1 - \alpha)\%$ lower and upper prediction bounds using GPQ-bootstrap method can be obtained by replacing the predictive distribution $G_{Y_n}^{DB}(\cdot|\cdot)$ with $G_{Y_n}^{GPQ}(\cdot|\cdot)$ in (6).

6.4 Coverage Probability of the Proposed Methods

This section shows that both the direct-bootstrap method (Section 6.2) and the GPQ-bootstrap method (Section 6.3) produce asymptotically correct prediction bounds/intervals for the future count Y_n . Hence, these two methods yield asymptotically valid inference for within-sample prediction of Y_n , as does the calibration-bootstrap method (Theorem 2, Section 5), but not by the standard plug-in method (Theorem 1, Section 4).

Theorem 3. *Under the same conditions as Theorem 2,*

1. The $100(1 - \alpha)\%$ upper and lower prediction bounds using the direct-bootstrap method, respectively $\tilde{Y}_{n,1-\alpha}^{DB}$ and $\underline{Y}_{n,1-\alpha}^{DB}$, have asymptotically correct coverage. That is,

$$\lim_{n \rightarrow \infty} \Pr(Y_n \leq \tilde{Y}_{n,1-\alpha}^{DB}) = 1 - \alpha = \lim_{n \rightarrow \infty} \Pr(Y_n \geq \underline{Y}_{n,1-\alpha}^{DB}).$$

2. If the parametric distribution $F(\cdot; \mu, \sigma)$ belongs to the log-location-scale distribution family (7), with standard cdf $\Phi(\cdot)$ differentiable on \mathbb{R} , the $100(1 - \alpha)\%$ upper and lower prediction bounds using the GPQ-bootstrap method, respectively $\tilde{Y}_{n,1-\alpha}^{GPQ}$ and $\underline{Y}_{n,1-\alpha}^{GPQ}$, have asymptotically correct coverage. That is,

$$\lim_{n \rightarrow \infty} \Pr(Y_n \leq \tilde{Y}_{n,1-\alpha}^{GPQ}) = 1 - \alpha = \lim_{n \rightarrow \infty} \Pr(Y_n \geq \underline{Y}_{n,1-\alpha}^{GPQ}).$$

The proof of Theorem 3 is in the online supplementary material.

7 Multiple Cohort Within-Sample Prediction

7.1 Multiple Cohort Data

So far, the focus has been on the within-sample prediction for single-cohort data. Multiple cohort data, however, are more common in applications. In this section, the results from single-cohort data are extended to multiple-cohort data.

In multiple-cohort data (e.g. the bearing cage data of Section 1), units from different cohorts are placed into service at different times. The multiple-cohort data \mathbb{D} can be seen as a collection of several single-cohort datasets as $\mathbb{D} = \{\mathbf{D}_{n_s}, s = 1, \dots, S\}$, where S is the number of cohorts and n_s is the number of units in the cohort s (sometimes, with no grouping, many cohorts have size 1). Within each cohort $\mathbf{D}_{n_s} = (D_{s,1}, \dots, D_{s,n_s})$, we may express an observation involved as $D_{s,i} = (\delta_i^s, T_i^{obs,s})$, for $T_i^{obs,s} = T_i^s \delta_i^s + (1 - \delta_i^s) t_c^s$, where T_i^s is a random variable from a parametric distribution $F(\cdot; \boldsymbol{\theta})$, t_c^s is the censoring time for cohort s , and $\delta_i^s = \mathbb{I}(T_i^s \leq t_c^s)$ is a random variable indicating whether a unit's value (e.g., failure time) is less than the censoring time t_c^s . Given the multiple-cohort data \mathbb{D} , the number of observed events (e.g., failures) within cohort s is defined as $r_{n_s} = \sum_{i=1}^{n_s} \mathbb{I}(T_i^s \leq t_c^s)$, $s = 1, \dots, S$, where the total number of units is $n = \sum_{s=1}^S n_s$. The predictand in the multiple-cohort data is the total number of events that will

occur in a future time window of length Δ and it is denoted by $Y_n = \sum_{s=1}^S \sum_{i=1}^{n_s} \mathbf{I}(t_c^s < T_i^s \leq t_w^s)$, where $t_w^s = t_c^s + \Delta$ for $s = 1, \dots, S$.

Within each cohort $s = 1, \dots, S$, the number $Y_s = \sum_{i=1}^{n_s} \mathbf{I}(t_c^s < T_i^s \leq t_w^s)$ of future events has a binomial distribution. As in Section 3, the conditional distribution of Y_s is $\text{binomial}(n - r_{n_s}, p_s)$, where p_s is defined as

$$p_s \equiv \pi_s(\boldsymbol{\theta}) = \frac{F(t_w^s; \boldsymbol{\theta}) - F(t_c^s; \boldsymbol{\theta})}{1 - F(t_c^s; \boldsymbol{\theta})}, \quad s = 1, \dots, S.$$

Consequently, the predictand $Y_n = \sum_{s=1}^S Y_s$ has a Poisson-binomial distribution with probability vector $\mathbf{p} = (p_1, \dots, p_S)$ and weight vector $\mathbf{w} = (n_1 - r_{n_1}, \dots, n_S - r_{n_S})$. We denote this Poisson-binomial distribution by $\text{Poibin}(\mathbf{p}, \mathbf{w})$, where the cdf of the Poisson-binomial distribution is denoted by $\text{ppoibin}(\cdot, \mathbf{p}, \mathbf{w})$ and the quantile function is denoted by $\text{qpoibin}(\cdot, \mathbf{p}, \mathbf{w})$; these functions are available in the **poibin** R package (described in Hong (2013)).

If $\hat{\boldsymbol{\theta}}_n$ is a consistent estimator of $\boldsymbol{\theta}$ based on the multiple-cohort data \mathbb{D} , an estimator $\hat{\mathbf{p}} = (\hat{p}_n^1, \dots, \hat{p}_n^S)$ of conditional probabilities \mathbf{p} follows by substitution $\hat{p}_n^s = \pi_s(\hat{\boldsymbol{\theta}}_n)$, $s = 1, \dots, S$, similar to the single-cohort case. Then, the $100(1 - \alpha)\%$ plug-in lower and upper prediction bounds for Y_n are

$$\begin{aligned} \tilde{Y}_{n,1-\alpha}^{PL} &= \sup\{y \in \{0\} \cup \mathbb{Z}^+ : \text{ppoibin}(y - 1, \hat{\mathbf{p}}, \mathbf{w}) \leq \alpha\} \\ &= \begin{cases} \text{qpoibin}(\alpha, \hat{\mathbf{p}}, \mathbf{w}), & \text{if } \text{pbinom}(\text{qpoibin}(\alpha, \hat{\mathbf{p}}, \mathbf{w}), \hat{\mathbf{p}}, \mathbf{w}) > \alpha, \\ \text{qpoibin}(\alpha, \hat{\mathbf{p}}, \mathbf{w}) + 1, & \text{if } \text{pbinom}(\text{qpoibin}(\alpha, \hat{\mathbf{p}}, \mathbf{w}), \hat{\mathbf{p}}, \mathbf{w}) = \alpha, \end{cases} \\ \tilde{Y}_{n,1-\alpha}^{PL} &= \inf\{y \in \{0\} \cup \mathbb{Z}^+ : \text{ppoibin}(y, \hat{\mathbf{p}}, \mathbf{w}) \geq 1 - \alpha\} = \text{qpoibin}(1 - \alpha, \hat{\mathbf{p}}, \mathbf{w}). \end{aligned}$$

Similar to the single-cohort case (Theorem 1), the plug-in method also fails to provide an asymptotically correct coverage probability under multiple-cohort data; see the online supplementary material.

7.2 The Calibration-Bootstrap Method for Multiple Cohort Data

Formulating prediction bounds using the calibration-bootstrap method first requires simulation of bootstrap samples, where each bootstrap sample \mathbb{D}^* matches the original data in terms of the number S of cohorts as well as their respective sizes n_s and censoring times t_c^s , $s = 1, \dots, S$. The bootstrap version of the estimator $\hat{\mathbf{p}} = (\hat{p}_n^1, \dots, \hat{p}_n^S)$ is $\hat{\mathbf{p}}^* = (\hat{p}_n^{1,*}, \dots, \hat{p}_n^{S,*})$ from each bootstrap sample \mathbb{D}^* . Additionally, the number of events (e.g., failures) in the bootstrap sample,

grouped by cohort, is $(r_{n_1}^*, \dots, r_{n_S}^*)$, from which we denote a bootstrap future count by $Y_n^\dagger \sim \text{Poibin}(\widehat{\mathbf{p}}; \mathbf{w}^*)$ based on a weight vector from the bootstrap sample as $\mathbf{w}^* = (n_1 - r_{n_1}^*, \dots, n_S - r_{n_S}^*)$. The bootstrap variable set $(Y_n^\dagger, \widehat{\mathbf{p}}^*, \mathbf{w}^*)$ is then applied into a Poisson-binomial cdf and then leads to a transformed random variable $U^* = \text{ppoibin}(Y_n^\dagger, \widehat{\mathbf{p}}^*, \mathbf{w}^*) \in [0, 1]$ for deriving calibrated confidence levels α_L^\dagger and α_U^\dagger in the same way as in the single-cohort situation. Then, the $100(1 - \alpha)\%$ calibrated lower prediction bound is $\underline{Y}_{n,1-\alpha}^C = \underline{Y}_{n,1-\alpha_L^\dagger}^{PL}$ and the similar upper prediction bound version is $\tilde{Y}_{n,1-\alpha}^C = \tilde{Y}_{n,1-\alpha_U^\dagger}^{PL}$.

The calibration-bootstrap method remains asymptotically correct for multiple-cohort within-sample prediction. The multiple-cohort extensions of Theorem 2 and the algorithm are in the online supplementary material.

7.3 The Direct- and GPQ-Bootstrap Methods for Multiple Cohort Data

For multiple-cohort data, constructing prediction bounds for Y_n based on the predictive-distribution-based methods also requires bootstrap data and, in particular, the distribution of a bootstrap version $\widehat{\mathbf{p}}^*$ of $\widehat{\mathbf{p}}$ as in Section 7.2. The predictive distribution from the direct-bootstrap method is

$$G_{Y_n}^{DB}(y|\mathbb{D}) = \int \text{ppoibin}(y, \widehat{\mathbf{p}}^*, \mathbf{w}) \Pr_*(d\widehat{\mathbf{p}}^*) \approx \frac{1}{B} \sum_{b=1}^B \text{ppoibin}(y, \widehat{\mathbf{p}}_b^*, \mathbf{w}). \quad (10)$$

where $\widehat{\mathbf{p}}_1^*, \dots, \widehat{\mathbf{p}}_B^*$ are realized bootstrap versions of $\widehat{\mathbf{p}}$ across independently generated bootstrap versions of multiple-cohort data (e.g., \mathbb{D}^*). The $100(1 - \alpha)\%$ direct-bootstrap lower and upper prediction bounds for Y_n are defined as the modified α quantile and $1 - \alpha$ quantile of this predictive distribution, respectively, and given by

$$\begin{aligned} \underline{Y}_{n,1-\alpha}^{DB} &= \sup \{y \in \{0\} \cup \mathbb{Z}^+ : G_{Y_n}^{DB}(y - 1|\mathbb{D}) \leq \alpha\}, \\ \tilde{Y}_{n,1-\alpha}^{DB} &= \inf \{y \in \{0\} \cup \mathbb{Z}^+ : G_{Y_n}^{DB}(y|\mathbb{D}) \geq 1 - \alpha\}. \end{aligned}$$

If $F(\cdot; \boldsymbol{\theta}) = F(\cdot; \mu, \sigma)$ belongs to the log-location-scale family as in (7), we use $\widehat{\boldsymbol{\theta}}_n^* = (\hat{\mu}_n^*, \hat{\sigma}_n^*)$ to compute approximate GPQs $\widehat{\boldsymbol{\theta}}_n^{**} = (\hat{\mu}_n^{**}, \hat{\sigma}_n^{**})$ using (9), and compute $\widehat{\mathbf{p}}^{**} = (\widehat{p}_n^{1,**}, \dots, \widehat{p}_n^{S,**})$ where $\widehat{p}_n^{s,**} = \pi_s(\widehat{\boldsymbol{\theta}}_n^{**})$. Then the GPQ-bootstrap method can be implemented to obtain prediction bounds for Y_n by replacing $\widehat{\mathbf{p}}^*$ with $\widehat{\mathbf{p}}^{**}$ in the definition of the direct-bootstrap predictive distribution (10) and analogously determining prediction bounds

from the quantiles of this predictive distribution. The direct- and GPQ-bootstrap methods produce asymptotically correct prediction bounds from multiple-cohort data, and the extension of Theorem 3 is provided in the online supplementary material.

8 A Simulation Study

The purpose of this simulation study is to illustrate agreement for finite sample sizes with the theorems established in the previous sections and to provide insights into the performance of different methods in the case of finite samples. The details and results in this section are for Type I censored single-cohort data. Let the event of interest be the failure of a unit. We simulated Type I censored data using the two-parameter Weibull distribution and compared the coverage probabilities of the prediction bounds based on the plug-in, calibration-bootstrap, direct-bootstrap, and GPQ-bootstrap methods. The Weibull cdf is

$$F(t; \eta, \beta) = 1 - \exp \left[- \left(\frac{t}{\eta} \right)^\beta \right], \quad t > 0,$$

with positive scale η and shape β parameters, and can also be parameterized as

$$F(t; \mu, \sigma) = \Phi_{\text{sev}} \left[\frac{\log(t) - \mu}{\sigma} \right], \quad t > 0,$$

where $\Phi_{\text{sev}}(x) = 1 - \exp[-\exp(x)]$ is the cdf of the standard smallest extreme value distribution with $\mu = \log(\eta)$ and $\sigma = 1/\beta$. The conditions in Theorems 1-3 can be verified for Type I censored Weibull data, so that the Weibull distribution can be used to illustrate all of the aforementioned methods for within-sample prediction (e.g., the ML estimators of the Weibull parameters $\hat{\theta}_n = (\hat{\mu}_n, \hat{\sigma}_n)$ have sampling distributions with normal limits and can be validly approximated by parametric bootstrap as described in Scholz (2001)).

8.1 Simulation Setup

The factors for the simulation experiment are (i) $p_{f1} = F(t_c; \beta, \eta)$, the probability that a unit fails before the censoring time t_c ; (ii) $E(r) = np_{f1}$, the expected number of failures at the censoring time t_c , where n is the total sample size (i.e., including both the censored and the uncensored observations); (iii) $d \equiv p_{f2} - p_{f1}$, the probability that a unit fails in a future time interval $(t_c, t_w]$ where $p_{f2} = F(t_w; \beta, \eta)$; (iv) $\beta = 1/\sigma$, the Weibull shape parameter. Because

$\eta = \exp(\mu)$ is a scale parameter, without loss of generality, $\eta = 1$ was used in the simulation. A simulation with all combinations of the following factors levels was conducted: (i) $p_{f1} = 0.05, 0.1, 0.2$; (ii) $E(r) = 5, 15, 25, 35, 45$; (iii) $d = 0.1, 0.2$; (iv) $\beta = 0.5, 0.8, 2, 4$.

For each combination of the these four factors, 90% and 95% upper prediction bounds and 90% and 95% lower prediction bounds were constructed.

The procedure for the simulation is as follows:

1. Simulate $N=5000$ Type I censored samples for each of the factors-level combinations of the four factors.
2. Use ML to estimate parameters β, η in each censored sample.
3. Compute prediction bounds using the different methods for each sample.
4. Compute the conditional (i.e., binomial) coverage probability for each of the prediction bounds.
5. Determine the unconditional coverage probability for each method by averaging the $N = 5000$ conditional coverage probabilities.

Within each of the $N=5000$ simulated Type I censored samples, $B=5000$ bootstrap samples were generated by parametric bootstrap (i.e., as a random sample from the fitted Weibull distribution with Type I censoring at t_c) and these samples were used for the calibration-bootstrap method and the two predictive-distribution-based methods. In the simulation, we excluded those samples having fewer than 2 failures to avoid estimability problems, so that all $N=5000$ original samples and all the $N \times B=25,000,000$ bootstrap samples in the simulation have at least 2 failures. The probability of a data sample with fewer than 2 failures for each factor-level combination is given in Table 1.

| | $E(r)=5$ | $E(r)=15$ | $E(r)=25$ | $E(r)=35$ | $E(r)=45$ |
|-----------------|----------|-----------|-----------|-----------|-----------|
| $p_{f1} = 0.05$ | 0.037 | 0.000 | 0.000 | 0.000 | 0.000 |
| $p_{f1} = 0.1$ | 0.034 | 0.000 | 0.000 | 0.000 | 0.000 |
| $p_{f1} = 0.2$ | 0.027 | 0.000 | 0.000 | 0.000 | 0.000 |

Table 1: Probability of an excluded sample (i.e., $r = 0$ or 1 failures) for different factor-level combinations.

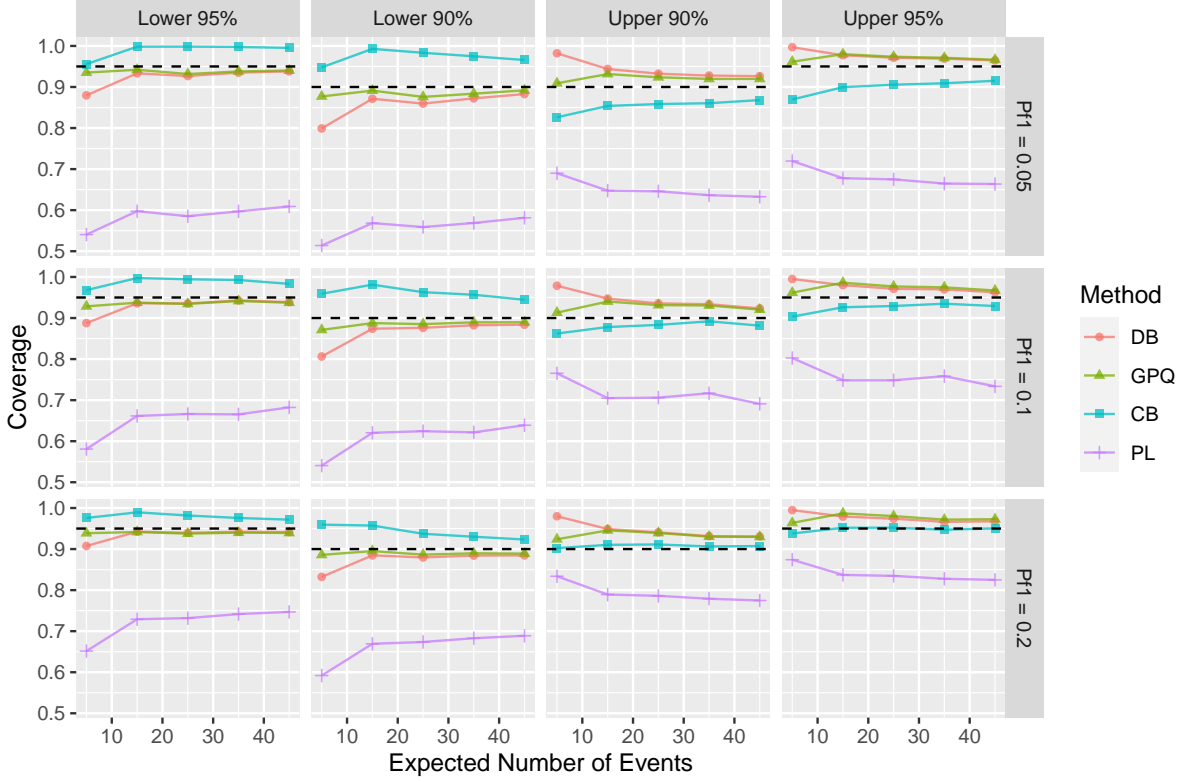


Figure 1: Coverage probabilities versus expected number of events for the direct-bootstrap (DB), GPQ-bootstrap (GPQ), calibration-bootstrap (CB), and plug-in (PL) methods when $d = p_{f2} - p_{f1} = 0.2$ and $\beta = 2$.

8.2 Simulation Results

A small subset of the plots displaying the complete simulation results are given here, as the results are generally consistent across the different factor-level combinations. Figure 1 shows the coverage probabilities from plug-in, calibration-bootstrap, direct-bootstrap, and GPQ-bootstrap methods when $\beta = 2$ and $d = 0.2$. The horizontal dashed line in each subplot represents the nominal confidence level. Plots for the other factor-level combinations are given in the online supplementary material.

Some observations from the simulation results are:

1. The plug-in method fails to have asymptotically correct coverage probability. As p_{f1} decreases, which entails less information or fewer events observed before the censoring time t_c , the coverage probability deviates more from the nominal level.
2. The direct- and GPQ-bootstrap methods are close to each other in terms of coverage probabilities except when $E(r) = 5$. The calibration-bootstrap method differs consid-

erably from the direct- and GPQ-bootstrap methods. The calibration-bootstrap method tends to be more conservative than the other bootstrap-based methods for constructing lower prediction bounds, and also is less conservative for constructing upper prediction bounds.

3. For the lower bounds, the direct- and GPQ-bootstrap methods dominate the calibration-bootstrap method. For the upper bounds, the coverage probabilities of the former two bootstrap-based methods are slightly conservative but still close to the nominal level. The calibration-bootstrap method is better than the direct- and GPQ-bootstrap methods in just a few of these upper bounds.
4. Compared with the calibration-bootstrap method, whose performance is highly related to the level of p_{f1} , the coverage probabilities of the direct- and GPQ-bootstrap methods are insensitive to the level of p_{f1} . As p_{f1} decreases, the lower prediction bound using the calibration-bootstrap method has over-coverage while the upper prediction bound has under-coverage. This implies that under heavy censoring (small p_{f1}), extremely large sample sizes n (or correspondingly large expected number of failing $E(r) = np_{f1}$) are required to attain coverage probabilities close to the nominal confidence level.

From these observations, we can see that the direct- and GPQ-bootstrap methods (i.e., predictive-distribution-based methods) tend to dominate the calibration-bootstrap method in terms of the performance of the prediction bounds, even though all three methods are asymptotically valid. This is because the predictive-distribution-based methods target the one source p of parameter uncertainty in the conditional binomial($n - r_n, p$) distribution of the predictand Y_n (i.e., as addressed by applying bootstrap versions \hat{p}^* or \hat{p}^{**} to “smooth” estimation uncertainty for p), while the number $n - r_n$ of Bernoulli trials used in these predictive distributions matches that of the predictand. Due to its definition, however, the calibration-bootstrap method involves bootstrap approximation steps (i.e., r_n^*, \hat{p}^*) for both the number r_n of failures as well as the binomial probability p . The calibration-bootstrap method essentially imposes an approximation $n - r_n^*$ for the known number $n - r_n$ of trials prescribing the predictand Y_n . As a consequence, coverages from the calibration-bootstrap method are generally less accurate than those from the predictive-distribution-based methods for within-sample prediction.

9 Application of the Methods

9.1 Examples

Product-A Data: The ML estimates of the Weibull shape and scale parameters are $\hat{\beta} = 1.518$ and $\hat{\eta} = 1152$, respectively, based on 80 failure times among 10,000 units before 48 months. Then, for the 9920 surviving units, the ML estimate of the probability that a unit will fail between 48 and 60 months of age is $\hat{p}_n = [F(60; \hat{\beta}, \hat{\eta}) - F(48; \hat{\beta}, \hat{\eta})] / [1 - F(48; \hat{\beta}, \hat{\eta})] = 0.00323$. Using the ML estimates of the Weibull parameters $(\hat{\beta}, \hat{\eta})$, we simulate 10,000 bootstrap samples that are censored at 48 months and obtain ML estimates of (β, η) from each bootstrap sample. Based on applying these with each interval method, Table 2 gives prediction bounds for the number of failures in the next 12 months. As indicated by our results, even with a large number of failures, the plug-in method intervals can be expected to be off and are too narrow compared to the other bounds.

| Confidence Level | Bound Type | Plug-in | Direct | GPQ | Calibration |
|------------------|------------|---------|--------|-----|-------------|
| 95% | Lower | 23 | 20 | 20 | 20 |
| 90% | Lower | 25 | 23 | 23 | 23 |
| 90% | Upper | 39 | 43 | 43 | 43 |
| 95% | Upper | 42 | 47 | 47 | 46 |

Table 2: Product A Data: Prediction Bounds for the number of failures in the next 12 months using different methods.

Heat Exchanger Data: In this example, there are no exact failure times in the data. That is, the data here contain limited information as there were only 8 failures among 20,000 exchanger tubes that were inspected (in censored data analysis, the informational content of data is closely related to the number of failures) and these failure times are interval-censored (not exact). The likelihood function under a Weibull model for the heat exchanger data is

$$L(\beta, \eta) = F(1; \beta, \eta)[F(2; \beta, \eta) - F(1; \beta, \eta)][F(3; \beta, \eta) - F(2; \beta, \eta)]^6[1 - F(3; \beta, \eta)]^{19992},$$

resulting in ML estimates $\hat{\beta} = 2.531$ and $\hat{\eta} = 66.058$. The conditional probability of a tube failing between the third and tenth year, given that tube has not failed at the end of the third year, is then estimated as $\hat{p}_n = [F(10; \hat{\beta}, \hat{\eta}) - F(3; \hat{\beta}, \hat{\eta})] / [1 - F(3; \hat{\beta}, \hat{\eta})] = 0.00797$.

The ML estimates from 10,000 bootstrap samples (parametric bootstrap with censoring at 3 years) are used in the calibration-bootstrap and two predictive-distribution-based methods.

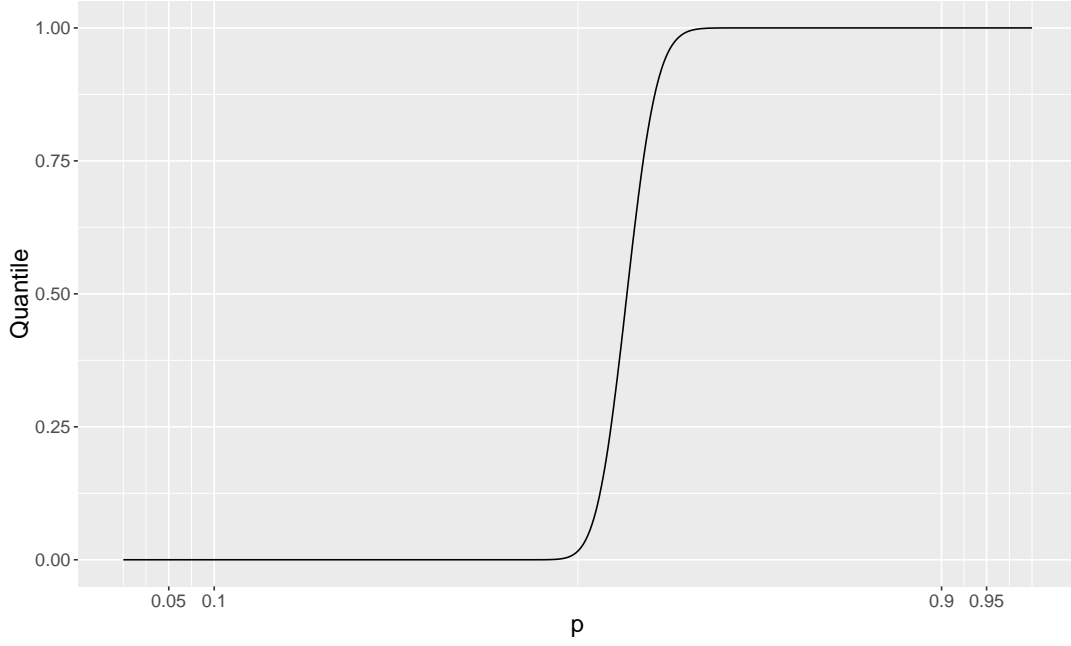


Figure 2: The quantile function of $\text{pbinom}(Y_n^\dagger, n - r_n^*, \hat{p}_n^*)$ used for the calibration-bootstrap method with heat exchanger data.

However, the calibration-bootstrap method exhibits numerical instabilities with these data due to the small number of failures. To illustrate, Figure 2 shows the approximate quantile function of $U^* = \text{pbinom}(Y_n^\dagger, n - r_n^*, \hat{p}_n^*)$ used in the calibration-bootstrap method, involving the evaluation of a $\text{binomial}(n - r_n^*, \hat{p}_n^*)$ random variable Y_n^\dagger in its cdf pbinom , given the number r_n^* of failures and the estimate \hat{p}_n^* from a bootstrap sample. This quantile function is also the calibration curve, where the x-axis gives the desired confidence level $1 - \alpha$, while the y-axis gives the corresponding calibrated confidence level (α_L^\dagger or $1 - \alpha_U^\dagger$) to be used for determining plug-in prediction bounds (or quantiles from a $\text{binomial}(n - r_n = 19992, \hat{p} = 0.00797)$ distribution). From Figure 2, we can see that the 0.05 and 0.1 quantiles nearly equal 0 while the 0.9 and 0.95 quantiles nearly equal 1. This creates complications in computing the prediction bounds, for example, as there is numerical instability near the 100% quantile of the $\text{binomial}(n - r_n = 19992, \hat{p} = 0.00797)$ distribution. Consequently, 90% and 95% bounds from the calibration-bootstrap method are computationally not available (NA). Table 3 instead provides prediction bounds from the plug-in and direct- and GPQ-bootstrap methods. The plug-in prediction bounds differ substantially from the two bootstrap-based methods. Unlike the previous example (Product A data), the direct- and GPQ-bootstrap methods also differ ap-

| Confidence Level | Bound Type | Plug-in | Direct | GPQ | Calibration |
|------------------|------------|---------|--------|------|-------------|
| 95% | Lower | 138 | 28 | 23 | NA |
| 90% | Lower | 142 | 43 | 34 | NA |
| 90% | Upper | 176 | 1627 | 888 | NA |
| 95% | Upper | 180 | 4343 | 1890 | NA |

Table 3: Heat Exchanger Data: Prediction Bounds for the number of failures in the next 7 years using different methods.

preciably based on the limited failure information with the heat exchanger data; we return to explore such differences in Section 9.2. The upper bounds involve a large amount of extrapolation and may not be practically meaningful other than to warn that there is a huge amount of uncertainty in the 10-year predictions.

Bearing Cage Data: In this example, staggered entry data containing multiple cohorts are considered. Table 4 gives the prediction bounds for the bearing cage dataset using 10,000 bootstrap samples. While similar in spirit to the Product-A example, the predictand here differs by having a Poisson-binomial distribution. The latter can be computed with the R package **poibin**, which is applied to construct prediction bounds using methods described in Section 7.2.

Table 4 gives the resulting prediction bounds for the bearing cage dataset.

| Confidence Level | Bound Type | Plug-in | Direct | GPQ | Calibration |
|------------------|------------|---------|--------|-----|-------------|
| 95% | Lower | 2 | 1 | 1 | 1 |
| 90% | Lower | 2 | 2 | 2 | 2 |
| 90% | Upper | 8 | 10 | 13 | 10 |
| 95% | Upper | 9 | 12 | 20 | 12 |

Table 4: Bearing Cage Data: Prediction Bounds for the number of failures in the next 300 service hours using different methods.

9.2 Comparing the Direct- and GPQ-Bootstrap Methods

In the heat exchanger example, the prediction bounds obtained from the direct- and GPQ-bootstrap methods appear very different. This motivates us to investigate the cause of such differences in similar prediction applications involving limited information.

A general simulation setting is first described for mimicking the heat exchanger data. The heat exchanger data has two important features in that the number of events is small (i.e., 8) and so is the proportion of observed events (i.e., 0.004). Hence, in the simulation, the

expected number of events $E(r)$ is set to 5 while the proportion failing p_{f1} is 0.001, with a Weibull shape parameter $\beta = 2$ and scale parameter $\eta = 1$. Different levels of $d = p_{f2} - p_{f1}$ are used for the probability of events in the forecast window. The simulation results (available in the online supplementary material) reveal that, overall, the GPQ-bootstrap method has better coverage probability than the direct-bootstrap method in this simulation setting. For the upper prediction bound, the direct-bootstrap method is generally more conservative than the GPQ-bootstrap method in terms of coverage probability, indicating that upper prediction bounds from the direct-bootstrap method are larger than the GPQ counterparts. On the other hand, the lower bound based on the direct-bootstrap method generally tends to have under-coverage compared to the GPQ-bootstrap method, suggesting also larger lower bounds from the direct-bootstrap method relative to the GPQ-bootstrap method. These patterns in the prediction bounds (i.e., with larger direct-bootstrap bounds compared to those from the GPQ-bootstrap in a setting of a limited number of events) are consistent with the prediction bounds found from the heat exchanger example. To further illustrate, Figure 3 shows the bootstrap

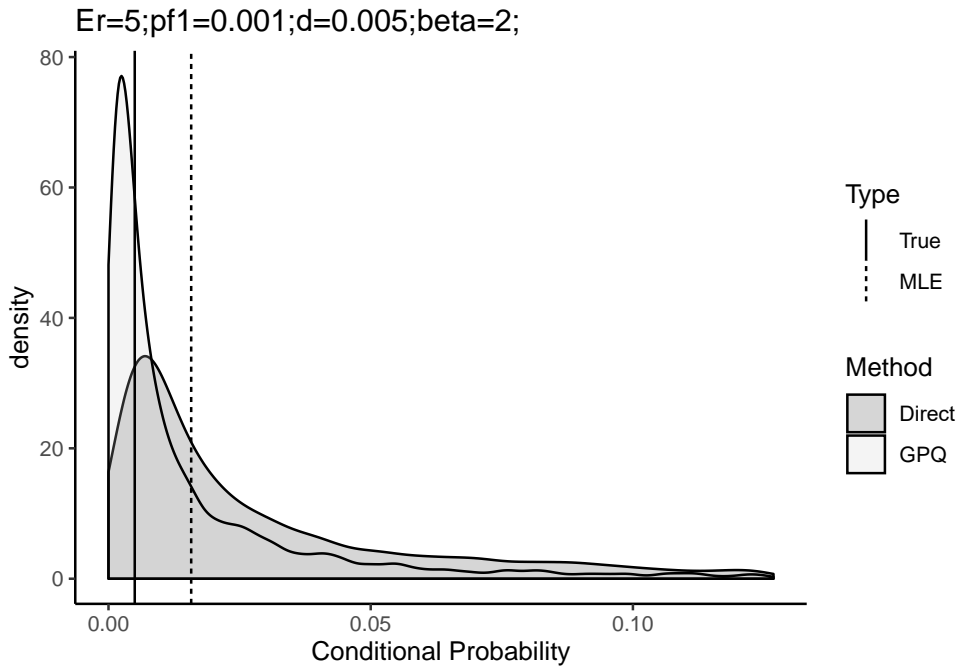


Figure 3: A Representative Distribution of \hat{p}^* and \hat{p}^{**} .

distributions of \hat{p}^* and \hat{p}^{**} from a single Monte Carlo sample that represents the typical behavior found in this simulation setting: values of \hat{p}^{**} used in the predictive distribution of GPQ-bootstrap method tend to be smaller and more concentrated than the \hat{p}^* values used

in the direct-bootstrap predictive distribution. Note that direct- and GPQ-bootstrap predictive distributions are approximated by $G_{Y_n}^{DB}(y|\mathbf{D}_n) \approx 1/B \sum_{b=1}^B \text{pbinom}(y, n - r_n, \hat{p}_b^*)$ and $G_{Y_n}^{GPQ}(y|\mathbf{D}_n) \approx 1/B \sum_{b=1}^B \text{pbinom}(y, n - r_n, \hat{p}_b^{**})$, respectively, and that direct- and GPQ-bootstrap prediction bounds correspond to quantiles from these predictive distributions. Consequently, because \hat{p}_b^* and \hat{p}_b^{**} are small (e.g., less than 0.25) while \hat{p}_b^* is generally larger than \hat{p}_b^{**} in Figure 3, then $G_{Y_n}^{DB}(y|\mathbf{D}_n)$ is generally smaller than $G_{Y_n}^{GPQ}(y|\mathbf{D}_n)$, implying quantiles from $G_{Y_n}^{DB}(y|\mathbf{D}_n)$ can be expected to exceed those from $G_{Y_n}^{GPQ}(y|\mathbf{D}_n)$ in data cases with a limited number of events. However, asymptotically, both \hat{p}_n^* and \hat{p}_n^{**} are similarly normally distributed and symmetric around \hat{p}_n (shown in online supplementary material), so that the direct- and GPQ-bootstrap prediction bounds may be expected to behave alike in data situations with a larger number of events and larger sample sizes, as seen in Figure 1 (and in the Product A application).

10 Choice of a Distribution

Extrapolation is usually required when predicting the number of future events based on an on-going time-to-event process. For example, it may be necessary to predict the number of returns in a three-year warranty period based on field data for the first year of operation of a product. An exception arises when life can be modeled in terms of use (as opposed to time in service) and there is much variability in use rates among units in the population. The high-use units will fail early and provide good information about the upper tail of the amount-of-use return-time distribution (e.g., Hong and Meeker (2010)).

When extrapolation is required, predictions can be strongly dependent on the distribution choice. In most applications, especially with heavy censoring, there is little or no useful information in the data to help choose a distribution. Then, for example, it is best to choose a failure-time distribution based on knowledge of the failure mechanism and the related physics/chemistry of failure. In important applications, this would be typically be done by consulting with experts who have such knowledge.

For example, the lognormal distribution could be justified for failure times that arise from the product of a large number of small, approximately independent positive random quanti-

ties. Examples include failure from crack initiation and growth due to cyclic stressing of metal components (e.g., in aircraft engines) and chemical degradation like corrosion (e.g., in microelectronics). These are two common applications where the lognormal distribution is often used. Gnedenko et al. (1969, pages 36-37) provide mathematical justification for this physical/chemical motivation.

Based on extreme value theory, the Weibull distribution can be used to model the distribution of the minimum of a large number of approximately iid positive random variables from certain classes of distributions. For example, the Weibull distribution may provide a suitable model for the time to first failure of a large number of similar components in a system. Consider a chain with many nominally identical links and suppose that the chain is subjected cyclic stresses over time. As suggested in the previous paragraph, the number of cycles to failure for each link could be described adequately with a lognormal distribution. The chain, however, fails when the first link fails. The limiting distribution of (properly standardized) minima of iid lognormal random variables is a type 1 smallest extreme value (or Gumbel) distribution. For all practical purposes, however, the Weibull distribution provides a better approximation. For further information on this result from the penultimate theory of extreme values, see Green (1976), Castillo (1988, Section 3.11), and Gomes and de Haan (1999). Similarly, if failures are driven by the maximum of a large number of approximately iid positive random variables, a Fréchet distribution would be suggested. The reciprocal of a Weibull random variable has a Fréchet distribution.

Of course, choosing a distribution based on failure-mechanism knowledge is not always possible. The alternative is to do sensitivity analyses, using different distributions. Figure 4 provides a comparison of the Weibull, lognormal, and Fréchet cdfs where the Weibull distribution was chosen with a shape parameter $\beta = 2$ and the other factor level combinations of p_{f1} and d used in the Section 8 simulation. The scale parameter η is determined by letting the 0.01 Weibull quantile be 1. The cdfs are plotted on lognormal probability scales where the lognormal cdf is a straight line. The particular parameters for the lognormal and Fréchet distributions were chosen such that the distributions cross at the 0.01 and p_{f1} quantiles, simulating the range of the data where the agreement among distributions will be good. Similar plots for $\beta = 1$ and

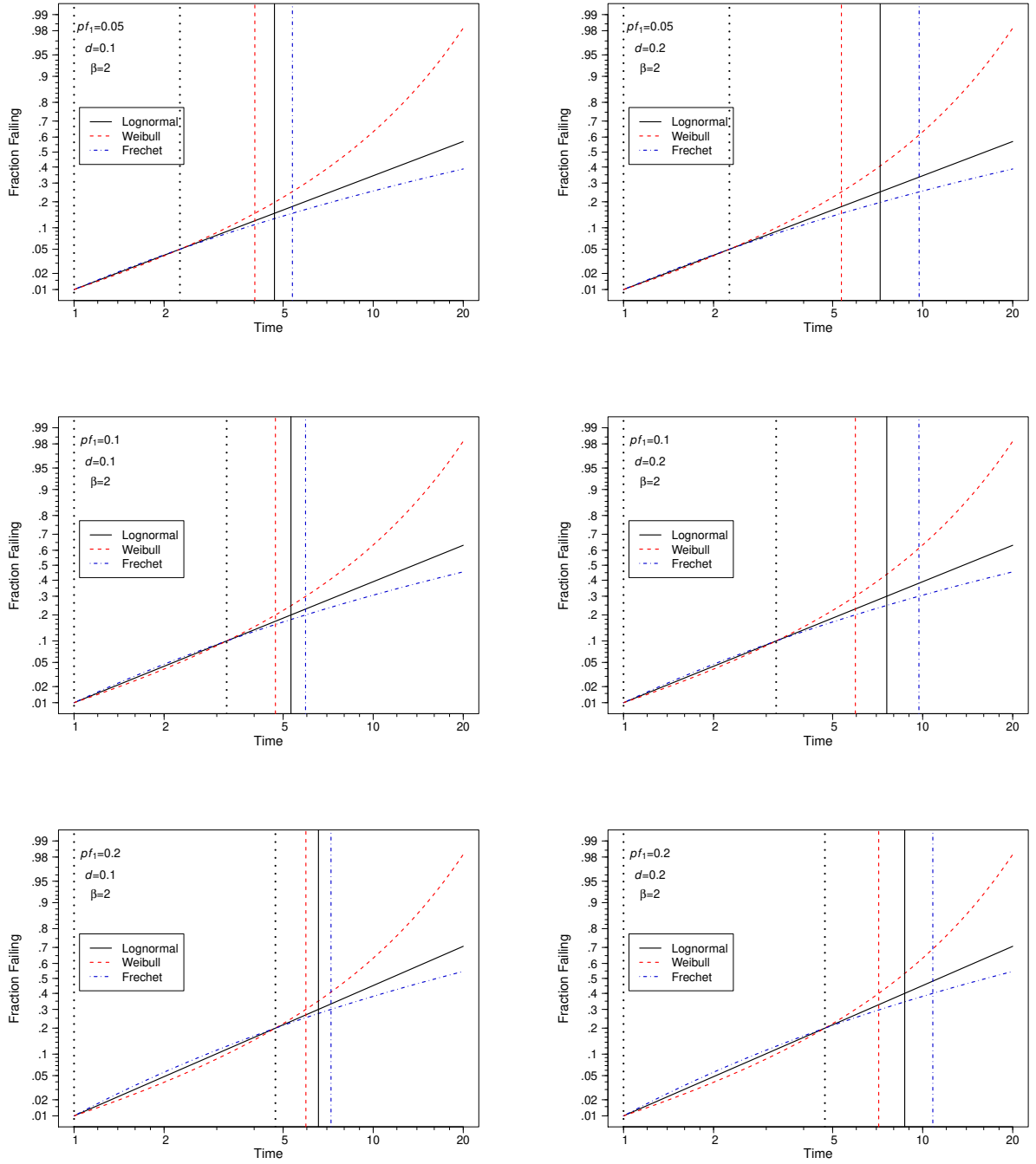


Figure 4: Distributional comparisons for $\beta = 2$. The two vertical dotted lines on the left indicate the points in time where all three distributions have the same 0.01 and p_{f1} quantiles. The three vertical lines on the right indicate the times at $p_{f2} = p_{f1} + d$ for the three distributions.

$\beta = 4$ are provided in the online supplementary material. The Weibull distribution is always more pessimistic (conservative) than the lognormal and the Fréchet is always more optimistic than the lognormal. For example, if the true distribution is Weibull but lognormal distribution is used to fit the data, the prediction intervals, regardless of the method, will underpredict

the number of events. When in doubt, the Weibull distribution is often used because it is the conservative choice.

11 Concluding Remarks

This paper studies the problem of predicting the future number of events based on censored time-to-event data (e.g., failure times). This type of prediction is known as within-sample prediction. A regular prediction problem is defined for which standard plug-in estimation commonly applies, and it is shown that the within-sample prediction is not regular and that the plug-in method fails to produce asymptotically valid prediction bounds. The irregularity of within-sample prediction and the failure of the plug-in method motivated the study of the calibration method as an alternative approach for prediction bounds, though the previously established theory for calibration bounds does not apply to within-sample prediction. The calibration method is implemented via bootstrap and called calibration-bootstrap method, which is proved to be asymptotically correct (i.e., producing prediction bounds with asymptotically correct coverage). Then, turning to formulations of a predictive distribution, we study and validate two other methods to obtain prediction bounds, namely the direct-bootstrap and GPQ-bootstrap methods. All prediction methods considered can be applied to both single-cohort and multiple-cohort data.

While theoretical results show that the calibration-bootstrap method and the two predictive-distribution-based methods are all asymptotically correct, the simulation study shows that the direct-bootstrap and GPQ-bootstrap methods outperform the calibration-bootstrap method in terms of coverage probability accuracy relative to a nominal coverage level. The two predictive-distribution-based methods are also easier to implement compared to the calibration-bootstrap method, and can also be computationally more stable (e.g., heat exchanger data example). Thus, we recommend predictive distribution methods, especially the direct-bootstrap method for general applications involving within-sample prediction.

In this paper, all of the units in the population were assumed to have the same time-to-event distributions. In many applications, however, units are exposed to different operating or environmental conditions, resulting in different time-to-event distributions. For example,

during 1996-2000, the Firestone tires installed on Ford Explorer SUVs experienced unusually high rates of failure, where problems first arose in Saudi Arabia, Qatar, and Kuwait because of the high temperatures in those countries (see National Highway Traffic Safety Administration (2001)). Having prediction intervals that use covariate information (like temperature and moisture) could be useful for manufacturers and regulators in making decisions about a possible product recall, for example. Similarly, there can be seasonality effects in time-to-event processes and within-sample predictions.

The methods described in this paper can be extended to handle either constant covariates or time-varying covariates. Using calibration-bootstrap methods, Hong et al. (2009) used constant covariates to predict power-transformer failures. Despite the complicated nature of their data (random right censoring and truncation and combinations of categorical covariates with small counts in some cells), Hong et al. (2009) were able to use the fractional random-weight method (e.g., Xu et al., 2020) to generate bootstrap estimates. Shan et al. (2020) used time-varying covariates to account for seasonality in two different warranty prediction applications. As mentioned by one of the referees, if there is seasonality and data from only part of one year is available, there is a difficulty. In such cases, it would be necessary to use past data on a similar process to provide information about the seasonality.

Covariate information in reliability field data has not been common, but that is changing, due to a reduction in costs and advances and in sensor, communications, and storage technology. In the future, much more covariate information on various system operating/environmental variables will be available to make better predictions, as described in Meeker and Hong (2014).

Acknowledgments

We would like to thank Luis A. Escobar for helpful comments on this paper. We are also grateful to the editorial staff, including two reviewers, for helpful comments that improved the manuscript. Research was partially supported by NSF DMS-2015390.

References

Abernethy, R., Breneman, J., Medlin, C., and Reinman, G. (1983). *Weibull Analysis Handbook*. Wright-Patterson AFB, Ohio 45433. Available at <https://apps.dtic.mil/dtic/>

tr/fulltext/u2/a143100.pdf. Last accessed on March 3, 2020.

- Aitchison, J. (1975). Goodness of prediction fit. *Biometrika*, 62:547–554.
- Atwood, C. L. (1984). Approximate tolerance intervals, based on maximum likelihood estimates. *Journal of the American Statistical Association*, 79:459–465.
- Barndorff-Nielsen, O. E. and Cox, D. R. (1996). Prediction and asymptotics. *Bernoulli*, 2:319–340.
- Beran, R. (1990). Calibrating prediction regions. *Journal of the American Statistical Association*, 85:715–723.
- Castillo, E. (1988). *Extreme Value Theory in Engineering (Statistical Modeling and Decision Science)*. Academic Press.
- Cox, D. R. (1975). Prediction intervals and empirical Bayes confidence intervals. *Journal of Applied Probability*, 12:47–55.
- Davison, A. C. (1986). Approximate predictive likelihood. *Biometrika*, 73:323–332.
- Escobar, L. A. and Meeker, W. Q. (1999). Statistical prediction based on censored life data. *Technometrics*, 41:113–124.
- Fonseca, G., Giummolè, F., and Vidoni, P. (2012). Calibrating predictive distributions. *Journal of Statistical Computation and Simulation*, 84:373–383.
- Gnedenko, B. V., Belyayev, Y. K., and Solov'yev, A. D. (1969). *Mathematical methods of reliability theory*. Academic Press.
- Gomes, M. I. and de Haan, L. (1999). Approximation by penultimate extreme value distributions. *Extremes*, 2:71–85.
- Green, R. F. (1976). Partial attraction of maxima. *Journal of Applied Probability*, 13:159–163.
- Hall, P., Peng, L., and Tajvidi, N. (1999). On prediction intervals based on predictive likelihood or bootstrap methods. *Biometrika*, 86:871–880.
- Hannig, J., Iyer, H., and Patterson, P. (2006). Fiducial generalized confidence intervals. *Journal of the American Statistical Association*, 101:254–269.
- Harris, I. R. (1989). Predictive fit for natural exponential families. *Biometrika*, 76:675–684.
- Hong, Y. (2013). On computing the distribution function for the Poisson-binomial distribution. *Computational Statistics and Data Analysis*, 59:41–51.
- Hong, Y. and Meeker, W. Q. (2010). Field-failure and warranty prediction based on auxiliary use-rate information. *Technometrics*, 52:148–159.
- Hong, Y. and Meeker, W. Q. (2013). Field-failure predictions based on failure-time data with dynamic covariate information. *Technometrics*, 55:135–149.

- Hong, Y., Meeker, W. Q., and McCalley, J. D. (2009). Prediction of remaining life of power transformers based on left truncated and right censored lifetime data. *The Annals of Applied Statistics*, 3:857–879.
- Lawless, J. F. and Fredette, M. (2005). Frequentist prediction intervals and predictive distributions. *Biometrika*, 92:529–542.
- Meeker, W. Q. and Hong, Y. (2014). Reliability meets big data: opportunities and challenges. *Quality Engineering*, 26:102–116.
- National Highway Traffic Safety Administration (2001). Engineering analysis report and initial decision regarding EA00-023: Firestone Wilderness AT Tires. *Washington, DC: US Department of Transportation*. Available at <https://icsw.nhtsa.gov/nhtsa/announce/press/Firestone/firestonesummary.html>. Last accessed on March 3, 2020.
- Nelson, W. (2000). Weibull prediction of a future number of failures. *Quality and Reliability Engineering International*, 16:23–26.
- Scholz, F. (2001). Maximum likelihood estimation for Type I censored Weibull data including covariates. In *ISSTECH-96-022, Boeing Information & Support Services, PO Box 24346, MS-7L-22*. Available at <http://faculty.washington.edu/fscholz/DATAFILES498B2008/ISSTECH-96-022.pdf>. Last accessed on August 3, 2020.
- Shan, Q., Hong, Y., and Meeker, W. Q. (2020). Seasonal warranty prediction based on recurrent event data. *Annals of Applied Statistics*, 14:929–955.
- Shen, J., Liu, R. Y., and Xie, M.-G. (2018). Prediction with confidence—a general framework for predictive inference. *Journal of Statistical Planning and Inference*, 195:126–140.
- Wang, C., Hannig, J., and Iyer, H. K. (2012). Fiducial prediction intervals. *Journal of Statistical Planning and Inference*, 142:1980–1990.
- Xie, M.-G. and Singh, K. (2013). Confidence distribution, the frequentist distribution estimator of a parameter: A review. *International Statistical Review*, 81:3–39.
- Xu, L., Gotwalt, C., Hong, Y., King, C. B., and Meeker, W. Q. (2020). Applications of the fractional-random-weight bootstrap. *The American Statistician*. <https://doi.org/10.1080/00031305.2020.1731599>.